

# Aerosol Water Content Drives Changes in Hydroxymethanesulfonate in Beijing Winter from 2015 to 2021

Yunzhi Xu,<sup>○</sup> Tao Ma,<sup>\*,○</sup> Haoqi Wang, Shaojie Song, Qipeng Qu, Shuxiao Wang, Jingkun Jiang, Xiaolin Duan, Xin Li, Guiqian Tang, Lidan Zhu, Qinqin Zhang, Yongliang Ma, Takashi Kimoto, Tao Huang, Taicheng An, Fengkui Duan,<sup>\*</sup> and Kebin He<sup>\*</sup>



Cite This: *Environ. Sci. Technol.* 2025, 59, 13903–13911



Read Online

ACCESS |

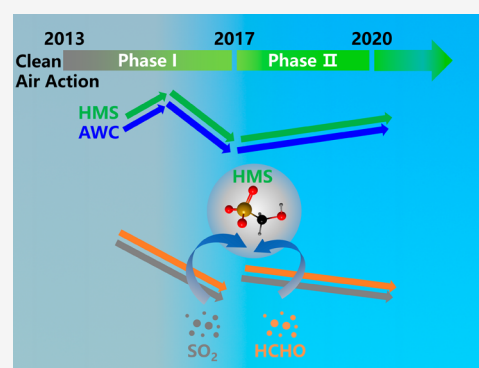
Metrics & More

Article Recommendations

Supporting Information

**ABSTRACT:** Hydroxymethanesulfonate (HMS) is an abundant secondary organosulfur aerosol during winter in the North China Plain, while the variation and affecting factors of HMS with implementing clean air actions remain unclear. Here, we conducted long-term field measurements in Beijing during the winter, including Phase I (2015–2017) and Phase II (2018–2021). Our results showed that HMS concentrations decreased significantly in Phase I, consistent with changes in  $PM_{2.5}$ , organic matter (OM), and sulfate, and showed an increasing trend in Phase II in contrast to the decreasing trend of  $PM_{2.5}$ , OM, and sulfate. In addition, HMS contributions to  $PM_{2.5}$ , OM, and particulate sulfur increased significantly during Phase II. HMS contributed up to 6% of  $PM_{2.5}$  and 24% of OM during heavy pollution periods in 2019. Despite the continuous reduction in gaseous precursors, the changes in aerosol water content driven by relative humidity and total chemical composition concentrations were the main factors influencing the interannual changes in HMS concentrations from 2015 to 2021 winter. Our findings highlight the importance of HMS during clean air actions and indicate that adverse meteorological conditions may somewhat offset the impact of precursor emission reductions on secondary aerosol formation.

**KEYWORDS:** hydroxymethanesulfonate, long-term variation, heterogeneous chemistry, aerosol water content



## 1. INTRODUCTION

Hydroxymethanesulfonate (HMS) is a ubiquitous organosulfur compound in aerosols around the world,<sup>1–9</sup> formed from dissolved  $SO_2$  and  $HCHO$ . Among them, the concentrations of HMS in particulate matter were higher in winter in northern China, which can be as high as  $18.5 \mu g m^{-3}$ .<sup>4,5,8</sup> HMS contributed a substantial mass of organic matter (OM)<sup>3,4</sup> and could be misidentified as sulfate in conventional aerosol mass spectrometry (AMS) and ion chromatography (IC) measurements.<sup>4,10</sup> Besides, the reaction of HMS with hydroxyl (OH) radicals in the aqueous phase is a potential source of sulfate.<sup>11–13</sup>

Previous studies of HMS have focused on short-term periods. With the implementation of the Air Pollution Prevention and Control Action Plan from 2013 to 2017 and the Three-Year Action Plan on Defending the Blue Sky from 2018 to 2020, the concentrations of particulate matter have decreased significantly due to the changes in anthropogenic emissions and meteorological conditions,<sup>14–16</sup> while the variation trends of various chemical components are different.<sup>17,18</sup> Some studies have investigated long-term variations of sulfate, nitrate, and organic aerosols (OA) and their response to the changes in emissions and meteorology<sup>17–19</sup> and have found widespread decreases in inorganic and organic aerosol concentrations. However, the secondary OA (SOA) mass fractions in OA increased from 49%

in 2013 to 61% in 2020.<sup>20</sup> As one of the typical SOA components, long-term changes in HMS during clean air actions are still poorly understood.

The factors affecting HMS formation are complex. The production medium of HMS in aerosols could be cloud water,<sup>21</sup> fog water,<sup>5,6</sup> and aerosol water.<sup>4,22,23</sup> The formation rate constant of HMS in high ionic strength aerosol water is several orders of magnitude higher than that in dilute cloud and fog water.<sup>24</sup> Considering the enhancement effect of the ionic strength on the HMS formation rate constant, the model simulation could better capture the variations of HMS.<sup>9,22,25</sup> HMS formation is highly dependent on pH, and the formation rate of HMS increases rapidly at higher pH values due to the increased dissociation of  $SO_2 \cdot H_2O$  into  $HSO_3^-$  and  $SO_3^{2-}$ .<sup>26</sup> The decomposition rate of HMS also increases rapidly with the increase of pH.<sup>27,28</sup> Field measurements have observed HMS in

**Received:** January 23, 2025

**Revised:** June 23, 2025

**Accepted:** June 25, 2025

**Published:** July 4, 2025



aerosols under moderate-pH conditions from 3 to 6.<sup>4,5,8,29,30</sup> Theoretically, high concentrations of gaseous precursors (SO<sub>2</sub> and HCHO), low atmospheric oxidizing capacity, low temperature, high water content, and moderately acid pH are favorable conditions for HMS formation and stability.<sup>3,4,23,25,31</sup> However, the main factors influencing the variation of HMS concentrations in the ambient atmosphere remain unclear.

In this study, we conducted winter field measurements of HMS and collocated instruments in Beijing from 2015 to 2021. We investigated the changes in HMS concentration and its importance during clean air actions. In addition, we analyzed the influence of gaseous precursors, atmospheric oxidants (e.g., O<sub>3</sub>), relative humidity (RH), temperature (*T*), aerosol water content (AWC), and pH on the variation of the HMS concentration and identified the key influencing factors of HMS formation in ambient aerosols.

## 2. MATERIALS AND METHODS

**2.1. Field Measurements.** We conducted offline sampling of PM<sub>2.5</sub> based on a low-volume air sampler (AS250D, Kimoto Electric Co., Ltd., Japan) and a medium-volume air sampler (Laoying 2030, Qingdao, China) in Tsinghua University (40.00° N, 116.34° E) in winter (November after municipal central heating, December, and the following January and February) from 2015 to 2021. The detailed sampling information is provided in Table S1 in the Supporting Information (SI). Hourly average PM<sub>2.5</sub> mass concentrations were measured with a PM-712 (Kimoto Electric Co., Ltd., Japan). Hourly concentrations of organic carbon (OC) in PM<sub>2.5</sub> were measured with a particulate carbon analyzer (APC-710; Kimoto Electric, Ltd., Japan), and the OM concentration was estimated as 1.6 times OC. Hourly concentrations of SO<sub>2</sub> were obtained by an online monitoring instrument SA-731 (Kimoto Electric Co., Ltd., Japan). Online HCHO measurement was conducted at the Chinese Academy of Meteorological Sciences by an Aero-Laser GmbH HCHO analyzer (model AL4021) in winter 2015,<sup>4</sup> Peking University by an Aero-Laser GmbH HCHO analyzer (model AL4021) in winter 2017,<sup>32</sup> and the Institute of Atmospheric Physics, Chinese Academy of Sciences by a proton transfer reaction-time-of-flight/mass spectrometry (PTR-TOF 4000, Ionicon, Austria) instrument in winter 2021.<sup>33</sup> The average HCHO concentration in winter of 2018 and 2019 was obtained from previous studies.<sup>32,33</sup> Hourly average *T* and RH were monitored with an automatic meteorological observation instrument (Milos 520, VAISALA Inc., Finland).

**2.2. HMS and Sulfate Quantification.** The detailed analysis method of HMS and sulfate has been described in our previous study.<sup>4,34</sup> For HMS and sulfate quantitation, 90 mm diameter quartz filters and 47 mm diameter quartz filters were cut by a 2 cm diameter circular punch and a quarter, respectively. Then, the cut filters were ultrasonically extracted twice with 5 mL of a 0.1% HCHO solution for 20 min each time and then filtered through 0.45 μm membrane syringe filters. The 0.1% HCHO solution was used to prevent S(IV) loss during pretreatment. Two extracts were combined for subsequent analysis in a Dionex Integration HPIC system. An AS11-HC analytical column and an AG11-HC guard column (Dionex Corp., CA) were used for the anion analysis. The eluent of 11 mM KOH with a flow rate of 1.5 mL min<sup>-1</sup> was used for the complete separation of S(IV) (i.e., HMS and other S(IV) species) and the sulfate peak. Previous parallel experiments with H<sub>2</sub>O<sub>2</sub> or HNO<sub>3</sub> solution to extract filter samples to isolate HMS

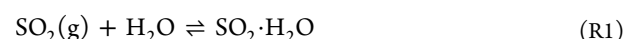
from free S(IV) showed that free S(IV) had a negligible influence on the HMS measurement in Beijing winter.<sup>8,5</sup> The UHPLC-LTQ-Orbitrap mass spectrometry method to quantify HMS concentration showed high reproducibility and agreement with the results by IC in Beijing winter.<sup>5</sup> Therefore, the IC method is a feasible technique for quantifying HMS in Beijing winter. It should be noted that the IC method may not be able to assume that the peak is exclusively HMS when applied to other regions, such as Fairbanks winters.<sup>35</sup>

**2.3. AWC and pH Calculations.** AWC and pH values were calculated by the thermodynamic model ISORROPIA-II.<sup>36–38</sup> Input data were attained by the online gas and aerosol monitoring instrument MARGA (Metrohm Ltd., Switzerland) at an hourly resolution on the campus of Tsinghua University. We used the forward model constrained by the measurements of gases (HNO<sub>3</sub>, HCl, and NH<sub>3</sub>) and aerosols (SO<sub>4</sub><sup>2-</sup>, NO<sub>3</sub><sup>-</sup>, Cl<sup>-</sup>, K<sup>+</sup>, Ca<sup>2+</sup>, Na<sup>+</sup>, Mg<sup>2+</sup>, and NH<sub>4</sub><sup>+</sup>), and we assumed the aerosol phase state to be metastable. The calculation of pH is described in Text S1. Considering that aerosols are unlikely to be completely liquid at low RH, data with RH < 20% were excluded when calculating pH.<sup>39</sup> The simulated NH<sub>3</sub>(g) and NH<sub>4</sub><sup>+</sup>(p) were in good agreement with the observations (Figure S1), indicating good performance of the ISORROPIA-II model in this study.

**2.4. Sensitivity of AWC.** To explore the major influencing factors on the AWC, sensitivity tests were performed by ISORROPIA-II. RH, *T*, SO<sub>4</sub><sup>2-</sup>, TNO<sub>3</sub> (HNO<sub>3</sub> + NO<sub>3</sub><sup>-</sup>), TNH<sub>3</sub> (NH<sub>3</sub> + NH<sub>4</sub><sup>+</sup>), and crustal ions (Ca<sup>2+</sup> + Mg<sup>2+</sup>) were selected as variables in the sensitivity analysis. The control variable method was applied to quantify the independent effects of specific parameters. Taking the effect of RH on AWC for example, RH is set as the actual observed series data, while all other input variables are fixed as the average values during the observation period to obtain the variations of AWC. The average value and variation range for each variable in different years are listed in Table S2. Relative standard deviation (RSD) was calculated to reflect the impact of variable variations on AWC. The higher the RSD, the greater the impact and vice versa.

**2.5. Kinetics of HMS Heterogeneous Production.** Based on kinetics, the HMS formation rate (*P*<sub>HMS</sub>) in aerosol water is calculated as follows.<sup>3</sup>

$$P_{\text{HMS}} = \frac{k_1 K_{s1} [\text{H}^+] + k_2 K_{s1} K_{s2}}{[\text{H}^+]^2} H_{\text{SO}_2} P_{\text{SO}_2} H_{\text{HCHO}} P_{\text{HCHO}} \text{AWC} \cdot M_{\text{HMS}} \quad (1)$$



Here, *k*<sub>1</sub> and *k*<sub>2</sub> are reaction rate constants for R5 and R6, respectively. *K*<sub>s1</sub> and *K*<sub>s2</sub> are acid dissociation constants for R2 and R3, respectively. *H*<sub>SO<sub>2</sub></sub> and *H*<sub>HCHO</sub> are Henry's law constants for SO<sub>2</sub> and HCHO, respectively. The above six parameters are temperature-related and need to be calculated according to the

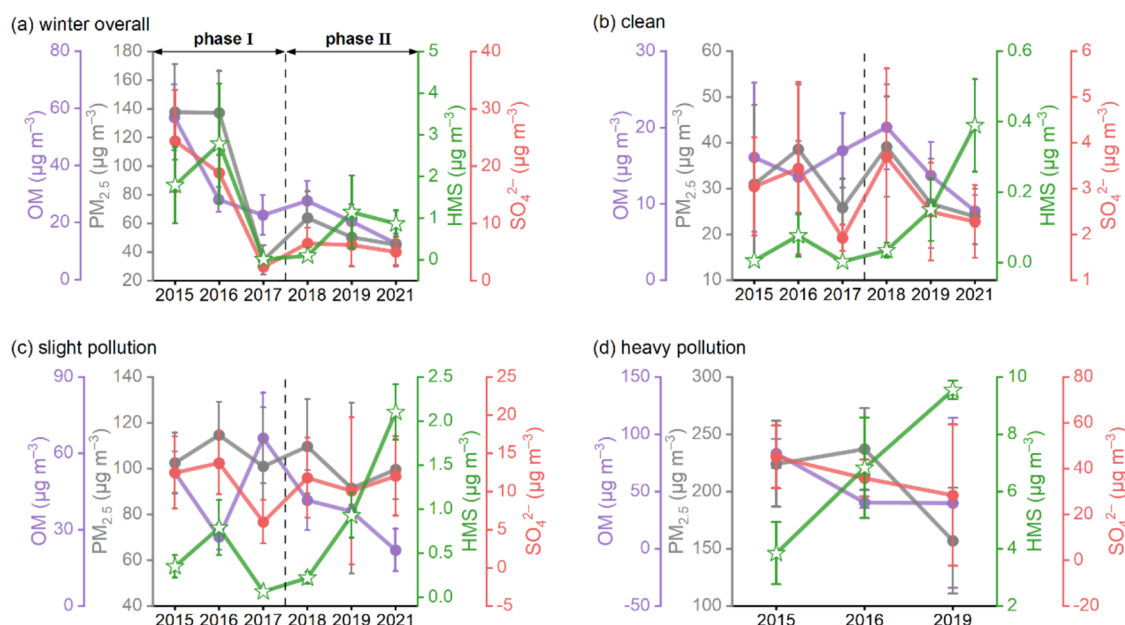


**Figure 1.** Variation of  $\text{PM}_{2.5}$ , OM, sulfate, and HMS mass concentrations in (a) overall winter, (b) clean periods, (c) slight pollution periods, and (d) heavy pollution periods from 2015 to 2021. The error bars represent the 95% confidence intervals of the mean.

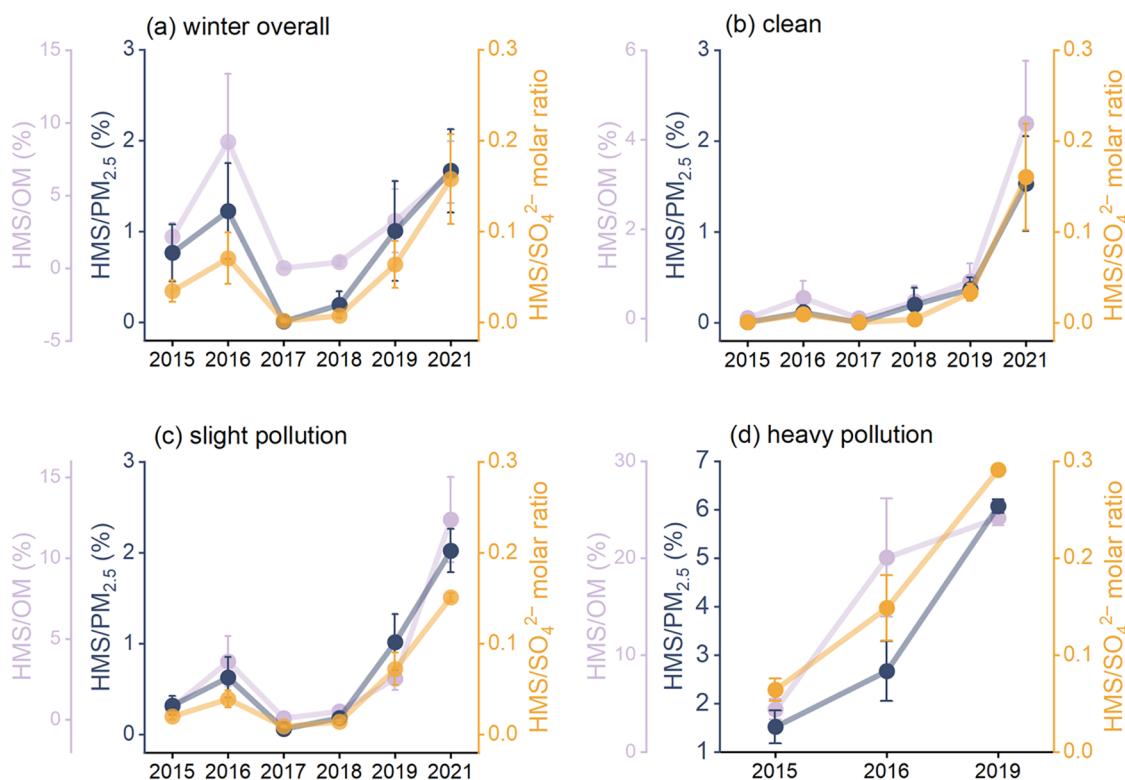


**Figure 2.** Variations of the HMS/ $\text{PM}_{2.5}$  mass ratio, HMS/OM mass ratio, and HMS/sulfate molar ratio in (a) overall winter, (b) clean samples, (c) slight pollution samples, and (d) heavy pollution samples from 2015 to 2021. The error bars represent the 95% confidence intervals of the mean.

actual temperature.  $P_{\text{SO}_2}$  and  $P_{\text{HCHO}}$  are partial pressures for  $\text{SO}_2$  and HCHO, respectively. AWC is the aerosol water content.  $M_{\text{HMS}}$  is the molar mass of the HMS.

### 3. RESULTS AND DISCUSSION

**3.1. Long-Term Variations of  $\text{PM}_{2.5}$ , OM, Sulfate, and HMS Concentrations.** Figure 1a shows the long-term variations of  $\text{PM}_{2.5}$ , OM, sulfate, and HMS in Beijing winter

from 2015 to 2021. With the implementation of clean air actions, the mean concentrations of  $\text{PM}_{2.5}$ , OM, sulfate, and HMS in Beijing winter reduced by 67%, 78%, 79%, and 51%, respectively, from 2015 to 2021. The detailed variation trend is different during Phase I (2015–2017) and Phase II (2018–2021), corresponding to the implementation of the Air Pollution Prevention and Control Action Plan and the Three-Year Action Plan on Defending the Blue Sky, respectively. In Phase I,  $\text{PM}_{2.5}$



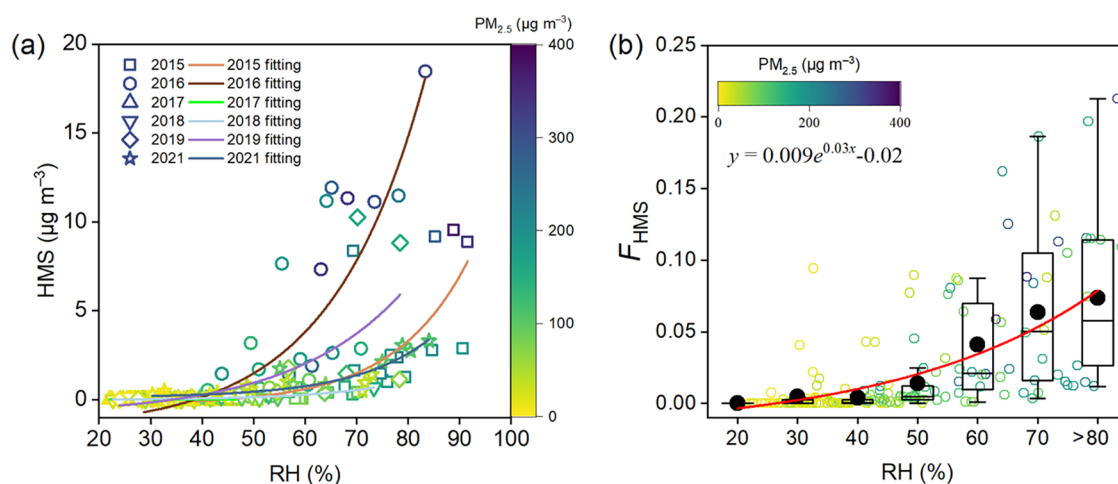


**Figure 3.** (a) Relationship between HMS concentration and RH in the winter of 2015–2021. The points are colored by  $\text{PM}_{2.5}$  concentrations. (b) Relationship between  $F_{\text{HMS}}$  and RH colored by  $\text{PM}_{2.5}$  concentrations. The data are binned according to RH (10% increment), and the median (middle horizontal line), mean (solid circles), 25th and 75th percentiles (lower and upper box), and 5th and 95th percentiles (lower and upper whiskers) are shown for each bin.

concentration dropped significantly from the high values in 2015 ( $137.8 \pm 93.1 \mu\text{g m}^{-3}$ ) and 2016 ( $137.2 \pm 92.9 \mu\text{g m}^{-3}$ ) to  $34.4 \pm 29.5 \mu\text{g m}^{-3}$  in 2017. After entering Phase II, the  $\text{PM}_{2.5}$  concentrations were in the low-value range and showed a slight downward trend year by year from  $63.8 \pm 39.5 \mu\text{g m}^{-3}$  in 2018 to  $45.1 \pm 36.9 \mu\text{g m}^{-3}$  in 2021. Geng et al. also reported an entire decreasing trend of  $\text{PM}_{2.5}$  concentration during the 2013–2020 period and a slower  $\text{PM}_{2.5}$  reduction rate during Phase II than during Phase I across China.<sup>16</sup> The reduction in OM and sulfate concentrations was mainly from Phase I, with a 60% and 90% reduction in 2017 compared to 2015, respectively. The rate of reduction slowed in Phase II, with a 54% and 23% reduction in 2021 compared to 2018. The variation of HMS was not consistent with that of  $\text{PM}_{2.5}$ , OM, and sulfate. The HMS concentration increased from  $1.79 \mu\text{g m}^{-3}$  in 2015 to  $2.79 \mu\text{g m}^{-3}$  in 2016 and then decreased to  $0.01 \mu\text{g m}^{-3}$  in 2017. Different from the declining trend of  $\text{PM}_{2.5}$ , OM, and sulfate concentrations in Phase II, HMS concentrations increased from 2018 to 2021.

The rising trend of HMS concentration in Phase II was more obvious under similar pollution levels. According to  $\text{PM}_{2.5}$  concentration, we classified the air quality into clean periods ( $\text{PM}_{2.5} \leq 75 \mu\text{g m}^{-3}$ ), slight pollution periods ( $75 \mu\text{g m}^{-3} < \text{PM}_{2.5} \leq 150 \mu\text{g m}^{-3}$ ), and heavy pollution periods ( $\text{PM}_{2.5} > 150 \mu\text{g m}^{-3}$ ). As shown in Figure S2, HMS concentrations increased with the deterioration of air quality, consistent with our previous study.<sup>4</sup> Therefore, the interannual upward trend of HMS from 2015 to 2021 was related to a reduction in the proportion of polluted samples (Figure S3). Figure 1b–d shows the interannual variation of  $\text{PM}_{2.5}$ , OM, sulfate, and HMS concentrations under three different pollution levels in Beijing winter. Under clean and slightly polluted conditions,  $\text{PM}_{2.5}$ , OM, and sulfate concentration showed a fluctuating variation, while HMS concentration showed a minor spike in 2016 and increased significantly in Phase II. In years with heavy pollution samples, HMS concentration also showed an upward trend from 2015 to 2019.

Figure 2 shows the interannual trend of the HMS contribution to  $\text{PM}_{2.5}$ , OM, and particulate sulfur. In general, the contributions of HMS to  $\text{PM}_{2.5}$  and OM mass and HMS/sulfate molar ratios spiked in 2016 in Phase I and increased significantly

in Phase II (Figure 2a). The interannual increase in the molar ratio of HMS to sulfate is consistent with the GEOS-Chem simulation,<sup>22</sup> indicating the increasing importance of HMS in particulate sulfur. In addition, the contribution of HMS to  $\text{PM}_{2.5}$  and OM mass and the molar ratio of HMS to sulfate increased with the aggravation of pollution (Figure S2). The proportion of HMS in  $\text{PM}_{2.5}$  and OM and the molar ratio of HMS to sulfate during clean, slight pollution, and heavy pollution periods (Figure 2b–d) showed interannual variation similar to that of HMS concentration. HMS contributed up to 6% of the  $\text{PM}_{2.5}$  mass and 24% of the OM mass under heavy pollution conditions in 2019.

**3.2. Drivers of Variation in HMS.** The formation of HMS in Beijing winter was associated with heterogeneous processes. Referring to previous studies,<sup>40</sup> here, we proposed a parameter,  $F_{\text{HMS}}$  (eq 2), to evaluate the fraction of HMS in total sulfur. HMS concentrations and  $F_{\text{HMS}}$  increased slowly at low RH (<50%) and accelerated at high RH above 50% (Figure 3). The exponential relationship between RH and HMS concentration,  $F_{\text{HMS}}$ , and the molar ratio of HMS to  $\text{SO}_2$  (Figure S4) suggests an important role of heterogeneous chemistry in HMS formation under wet conditions.<sup>40,41</sup> The rate of change in HMS with RH varied across years, with faster changes in the winter of 2016, 2019, and 2015. We further investigated the effects of cloud/fog events on HMS formation and found that the frequency of clouds and fogs in Beijing winter was low, and the correlation between cloud/fog liquid water content (LWC) and HMS concentration was insignificant (Figure S5,  $P > 0.05$ ), suggesting that the cloud/fog process may be less important than aqueous aerosol processes for HMS production in Beijing winter. Recent studies have also indicated the critical role of aqueous aerosol chemistry in HMS formation in regions where cloud liquid water is scarce.<sup>23</sup>

$$F_{\text{HMS}} = \frac{n[\text{HMS}]}{n[\text{HMS}] + n[\text{SO}_4^{2-}] + n[\text{SO}_2]} \quad (2)$$

Here,  $n[\text{HMS}]$ ,  $n[\text{SO}_4^{2-}]$ , and  $n[\text{SO}_2]$  refer to the molar concentrations of HMS,  $\text{SO}_4^{2-}$ , and  $\text{SO}_2$ , respectively.

To identify the key parameters that affect the formation of HMS in ambient air, we investigated the correlation between HMS concentration and influencing factors in the winter from

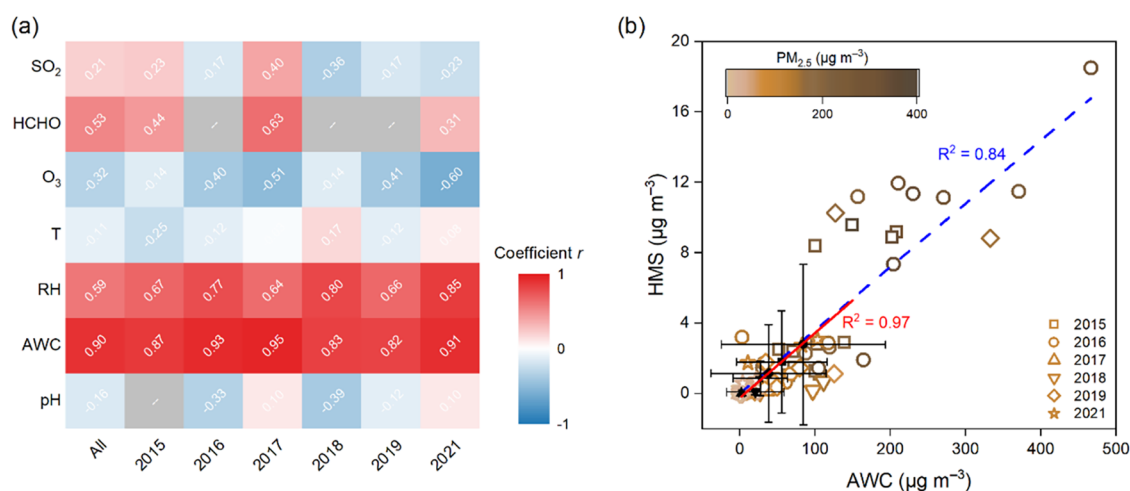


**Figure 4.** (a) Pearson  $r$  values for the correlations between HMS concentration and major influencing factors in the winter from 2015 to 2021. (b) Relationship between HMS concentration and AWC, colored by the PM<sub>2.5</sub> concentration. Solid black dots represent annual averages. The solid red line fits the annual mean, and the dashed blue line fits the sample data points.

2015 to 2021 (Figure 4a). Theoretically, high concentrations of precursors (SO<sub>2</sub> and HCHO), low oxidant levels, low temperature, high RH, and pH favor the HMS formation.<sup>4,42–44</sup> AWC and RH correlated strongly and positively ( $r = 0.59–0.95$ ,  $P < 0.0001$ ) with HMS concentration, consistent with previous studies,<sup>4</sup> indicating that aerosol water serves as a medium for the formation of HMS. High RH conditions were usually accompanied by rapid secondary chemical processes in Beijing haze.<sup>40,41</sup> Rural HMS at the Gucheng site was higher than that at the urban site Beijing due to the higher RH.<sup>8</sup> HMS concentration correlated well with HCHO concentration ( $r = 0.31–0.63$ ,  $P < 0.05$ ), while the relationship between HMS and SO<sub>2</sub> concentration was insignificant ( $P > 0.05$ ), suggesting the importance of HCHO concentration on HMS formation.<sup>21,35</sup> HMS concentration showed a negative correlation with O<sub>3</sub> concentration ( $P < 0.05$ ). Because HMS formation competes with S(IV) oxidation reactions, low oxidants may reduce the oxidation of S(IV) and facilitate the formation of HMS.<sup>4,22,25</sup> In addition, HMS could be oxidized by OH radicals to form sulfate,<sup>12</sup> and low oxidants were unfavorable for the heterogeneous oxidation of HMS.<sup>22</sup> The correlation between temperature, pH, and HMS concentration was insignificant ( $P > 0.05$ ). From the perspective of daily changes in HMS concentration, AWC was the key factor affecting the concentration of HMS, followed by RH.

We further studied the interannual variation of the factors influencing HMS formation and found that AWC showed the best agreement with the interannual variation in HMS concentrations (Figure S6). The concentration of SO<sub>2</sub> in Beijing winter continued to decline from  $9.7 \pm 4.4$  ppb in 2015 to  $1.1 \pm 0.3$  ppb in 2021 (Figure S6b), consistent with the variation trend of SO<sub>2</sub> reported in northern China.<sup>45</sup> The reduction in SO<sub>2</sub> concentration was mainly attributed to the implementation of strict desulfurization measures in power plants and emission-intensive industrial sectors.<sup>14</sup> The interannual variation of HCHO also showed a downward trend (Figure S6c). The decrease in the concentration of precursors could not explain the increase in HMS concentration in Phase II mentioned above. O<sub>3</sub> concentration showed an interannual increasing trend (Figure S6b), which is unfavorable for HMS formation. The interannual variation trend of RH was almost consistent with that of the HMS concentration in Phase II

(Figure S6d). The interannual variation trend of AWC (Figure S6e) agreed well with the trend in HMS concentration, while the variation trend of LWC and HMS concentrations was not consistent (Figure S6a). As shown in Figure 4b, the annual average HMS concentration correlated well with the AWC ( $R^2 = 0.97$ ). The pH of aerosol in Beijing in winter fluctuated in the range of 4–5.5 (Figure S6e). Theoretically, high pH facilitated the formation of HMS, since high pH favored the dissociation of SO<sub>2</sub>·H<sub>2</sub>O into HSO<sub>3</sub><sup>−</sup> and SO<sub>3</sub><sup>2−</sup>.<sup>3,31</sup> Moderately acidic pH in Beijing winter haze favored the HMS formation and prevented the HMS decomposition.<sup>3</sup> In the real atmosphere, the interannual variation of the pH could not explain the observed variation of HMS concentrations. In addition, the calculated heterogeneous HMS formation rate (Figure S7) in 2015, 2017, and 2021 was consistent with the variation of HMS concentration, implying the importance of heterogeneous chemistry on HMS formation.

Figure S8 shows the effects of RH,  $T$ , total chemical compositions, SO<sub>4</sub><sup>2−</sup>, TNO<sub>3</sub>, TNH<sub>3</sub>, and crustal ions on AWC through sensitivity analysis using the ISORROPIA-II model. In the sensitivity test, AWC showed an exponential relationship with RH (Figure S8a). Temperature exhibited an opposite trend to AWC (Figure S8b), indicating the inhibitory effect of temperature on AWC. The total concentration of chemical compositions showed a linear relationship with AWC (Figure S8c). Based on the RSD analysis in Table S3, RH and total concentration of chemical compositions were the two factors with higher RSD, reflecting their strong influence on AWC. We then studied the effect of individual chemical components on AWC (Figure S8d–g). AWC increased with the concentrations of SO<sub>4</sub><sup>2−</sup>, TNO<sub>3</sub>, and TNH<sub>3</sub>, while crustal ions Ca<sup>2+</sup> and Mg<sup>2+</sup> showed a minor negative effect on AWC. The impact of SO<sub>4</sub><sup>2−</sup> on AWC was significant in 2016, while the impact of TNO<sub>3</sub> and TNH<sub>3</sub> on AWC gradually increased and exceeded that of SO<sub>4</sub><sup>2−</sup> since 2017. As the dominant ions in PM<sub>2.5</sub> shifted from sulfate to nitrate after 2017,<sup>46</sup> nitrate became the main driver of AWC increase.<sup>47</sup> The interannual variation of AWC was similar to that of RH and the total concentration of chemical compositions (Figure S6). In general, the driving factors affecting AWC variations in winter from 2015 to 2021 were the RH and total concentration of chemical compositions.

**3.3. Atmospheric Implications.** Our field measurements reveal the long-term variation of HMS in Beijing winter during clean air actions. HMS showed growing importance in Phase II in terms of concentration and contribution to  $\text{PM}_{2.5}$ , OM, and particulate sulfur. Primary emissions, secondary formation, and adverse meteorological conditions affected the formation of particulate matter.<sup>41,48,49</sup> During clean air actions, the significant reductions in anthropogenic emissions drove the improvement of air quality in China.<sup>16</sup> However, enhanced secondary formation accompanied by adverse meteorological conditions may exacerbate particulate matter pollution.<sup>50</sup> HMS can be used as a marker for secondary processing in the aqueous/heterogeneous phase.<sup>23</sup> Despite the decreases in precursors ( $\text{SO}_2$  and  $\text{HCHO}$ ), the growing importance of HMS indicates that secondary formation under adverse meteorological conditions may somewhat offset the impact of primary emission reductions on particulate matter mitigation.

This study demonstrates the important role of AWC in HMS formation in Beijing winter. Factors affecting HMS changes in the atmosphere are complex. Aerosol water is an important component of atmospheric aerosols, which serves as a medium that enables aqueous-phase reactions.<sup>51</sup> AWC is the key factor affecting HMS variation in Beijing winter, and RH and chemical components determine the AWC.<sup>47</sup> Experimental and model studies also confirmed that aerosol water plays an important role in HMS chemistry during haze in China.<sup>22,24</sup> Previous model results showed that atmospheric acidity was a critical factor in HMS variation.<sup>22,31</sup> Actually, the field measurements show that aerosol acidity during winter in the North China Plain is relatively stable, with pH values ranging from 4 to 5.<sup>3,4,52,53</sup> In this study, the fluctuating pH value in Beijing winter cannot explain the changes in HMS. In Alaska, low temperatures can play a role through a unique effect on pH that enables substantial HMS production.<sup>23</sup> In the future, more field, laboratory, and modeling research is needed to study the key factors influencing the formation of HMS in different regions of the world.<sup>35</sup>

## ■ ASSOCIATED CONTENT

### SI Supporting Information

The Supporting Information is available free of charge at <https://pubs.acs.org/doi/10.1021/acs.est.5c01170>.

Details of aerosol pH calculation (Text S1); ISORROPIA-II validation (Figure S1); sampling information (Figure S3 and Table S1); AWC sensitivity test (Figure S8 and Tables S2 and S3); and additional figures on HMS and related parameters (Figures S2 and S4–S7) (PDF)

## ■ AUTHOR INFORMATION

### Corresponding Authors

**Tao Ma** — Guangdong-Hong Kong-Macao Joint Laboratory for Contaminants Exposure and Health, Guangdong Key Laboratory of Environmental Catalysis and Health Risk Control, Institute of Environmental Health and Pollution Control, Guangdong University of Technology, Guangzhou 510006, China; Guangdong Basic Research Center of Excellence for Ecological Security and Green Development, Key Laboratory of City Cluster Environmental Safety and Green Development of the Ministry of Education, School of Environmental Science and Engineering, Guangdong University of Technology, Guangzhou 510006, China; Email: [matao@gdut.edu.cn](mailto:matao@gdut.edu.cn)

**Fengkui Duan** — State Key Laboratory of Regional Environment and Sustainability, School of Environment, State Environmental Protection Key Laboratory of Sources and Control of Air Pollution Complex, Beijing Key Laboratory of Indoor Air Quality Evaluation and Control, Tsinghua University, Beijing 100084, China; [orcid.org/0000-0002-5501-6048](https://orcid.org/0000-0002-5501-6048); Email: [duanfku@tsinghua.edu.cn](mailto:duanfku@tsinghua.edu.cn)

**Kebin He** — State Key Laboratory of Regional Environment and Sustainability, School of Environment, State Environmental Protection Key Laboratory of Sources and Control of Air Pollution Complex, Beijing Key Laboratory of Indoor Air Quality Evaluation and Control, Tsinghua University, Beijing 100084, China; Email: [hekb@tsinghua.edu.cn](mailto:hekb@tsinghua.edu.cn)

### Authors

**Yunzhi Xu** — State Key Laboratory of Regional Environment and Sustainability, School of Environment, State Environmental Protection Key Laboratory of Sources and Control of Air Pollution Complex, Beijing Key Laboratory of Indoor Air Quality Evaluation and Control, Tsinghua University, Beijing 100084, China

**Haoqi Wang** — State Environmental Protection Key Laboratory of Urban Ambient Air Particulate Matter Pollution Prevention and Control, College of Environmental Science and Engineering, Nankai University, Tianjin 300350, China; [orcid.org/0000-0001-9002-0774](https://orcid.org/0000-0001-9002-0774)

**Shaojie Song** — State Environmental Protection Key Laboratory of Urban Ambient Air Particulate Matter Pollution Prevention and Control, College of Environmental Science and Engineering, Nankai University, Tianjin 300350, China; [orcid.org/0000-0001-6395-7422](https://orcid.org/0000-0001-6395-7422)

**Qipeng Qu** — State Key Laboratory of Regional Environment and Sustainability, School of Environment, State Environmental Protection Key Laboratory of Sources and Control of Air Pollution Complex, Beijing Key Laboratory of Indoor Air Quality Evaluation and Control, Tsinghua University, Beijing 100084, China

**Shuxiao Wang** — State Key Laboratory of Regional Environment and Sustainability, School of Environment, State Environmental Protection Key Laboratory of Sources and Control of Air Pollution Complex, Beijing Key Laboratory of Indoor Air Quality Evaluation and Control, Tsinghua University, Beijing 100084, China; [orcid.org/0000-0001-9727-1963](https://orcid.org/0000-0001-9727-1963)

**Jingkun Jiang** — State Key Laboratory of Regional Environment and Sustainability, School of Environment, State Environmental Protection Key Laboratory of Sources and Control of Air Pollution Complex, Beijing Key Laboratory of Indoor Air Quality Evaluation and Control, Tsinghua University, Beijing 100084, China

**Xiaolin Duan** — State Key Laboratory of Regional Environment and Sustainability, School of Environment, State Environmental Protection Key Laboratory of Sources and Control of Air Pollution Complex, Beijing Key Laboratory of Indoor Air Quality Evaluation and Control, Tsinghua University, Beijing 100084, China

**Xin Li** — State Key Laboratory of Regional Environment and Sustainability, College of Environmental Sciences and Engineering, Peking University, Beijing 100871, China; [orcid.org/0000-0001-5129-4801](https://orcid.org/0000-0001-5129-4801)

**Guiqian Tang** — State Key Laboratory of Atmospheric Environment and Extreme Meteorology, Institute of



Atmospheric Physics, Chinese Academy of Sciences, Beijing 100049, China; [orcid.org/0000-0002-4381-5344](https://orcid.org/0000-0002-4381-5344)

**Lidan Zhu** – State Key Laboratory of Regional Environment and Sustainability, School of Environment, State Environmental Protection Key Laboratory of Sources and Control of Air Pollution Complex, Beijing Key Laboratory of Indoor Air Quality Evaluation and Control, Tsinghua University, Beijing 100084, China

**Qinqin Zhang** – State Key Laboratory of Regional Environment and Sustainability, School of Environment, State Environmental Protection Key Laboratory of Sources and Control of Air Pollution Complex, Beijing Key Laboratory of Indoor Air Quality Evaluation and Control, Tsinghua University, Beijing 100084, China

**Yongliang Ma** – State Key Laboratory of Regional Environment and Sustainability, School of Environment, State Environmental Protection Key Laboratory of Sources and Control of Air Pollution Complex, Beijing Key Laboratory of Indoor Air Quality Evaluation and Control, Tsinghua University, Beijing 100084, China

**Takashi Kimoto** – Kimoto Electric Co., Ltd., Osaka 543-0024, Japan

**Tao Huang** – Kimoto Electric Co., Ltd., Osaka 543-0024, Japan

**Taicheng An** – Guangdong-Hong Kong-Macao Joint Laboratory for Contaminants Exposure and Health, Guangdong Key Laboratory of Environmental Catalysis and Health Risk Control, Institute of Environmental Health and Pollution Control, Guangdong University of Technology, Guangzhou 510006, China; Guangdong Basic Research Center of Excellence for Ecological Security and Green Development, Key Laboratory of City Cluster Environmental Safety and Green Development of the Ministry of Education, School of Environmental Science and Engineering, Guangdong University of Technology, Guangzhou 510006, China

Complete contact information is available at:  
<https://pubs.acs.org/10.1021/acs.est.5c01170>

## Author Contributions

<sup>○</sup>Y.X. and T.M. contributed equally to this work.

## Notes

The authors declare no competing financial interest.

## ACKNOWLEDGMENTS

This work is supported by the National Natural Science Foundation of China (22188102 and 22206098), National Key R & D Program of China (2022YFE0105500), special fund of State Key Laboratory of Regional Environment and Sustainability (24K13ESPCT), and Natural Science Foundation of Tianjin City (22JCYBJC01330).

## REFERENCES

- (1) Scheinhardt, S.; van Pinxteren, D.; Müller, K.; Spindler, G.; Herrmann, H. Hydroxymethanesulfonic acid in size-segregated aerosol particles at nine sites in Germany. *Atmos. Chem. Phys.* **2014**, *14* (9), 4531–4538.
- (2) Gilardoni, S.; Massoli, P.; Paglione, M.; Giulianelli, L.; Carbone, C.; Rinaldi, M.; Decesari, S.; Sandrini, S.; Costabile, F.; Gobbi, G. P.; Pietrogrande, M. C.; Visentin, M.; Scotto, F.; Fuzzi, S.; Facchini, M. C. Direct observation of aqueous secondary organic aerosol from biomass-burning emissions. *Proc. Natl. Acad. Sci. U.S.A.* **2016**, *113* (36), 10013–10018.
- (3) Song, S.; Gao, M.; Xu, W.; Sun, Y.; Worsnop, D. R.; Jayne, J. T.; Zhang, Y.; Zhu, L.; Li, M.; Zhou, Z.; Cheng, C.; Lv, Y.; Wang, Y.; Peng,

W.; Xu, X.; Lin, N.; Wang, Y.; Wang, S.; Munger, J. W.; Jacob, D. J.; McElroy, M. B. Possible heterogeneous chemistry of hydroxymethanesulfonate (HMS) in northern China winter haze. *Atmos. Chem. Phys.* **2019**, *19* (2), 1357–1371.

(4) Ma, T.; Furutani, H.; Duan, F.; Kimoto, T.; Jiang, J.; Zhang, Q.; Xu, X.; Wang, Y.; Gao, J.; Geng, G.; Li, M.; Song, S.; Ma, Y.; Che, F.; Wang, J.; Zhu, L.; Huang, T.; Toyoda, M.; He, K. Contribution of hydroxymethanesulfonate (HMS) to severe winter haze in the North China Plain. *Atmos. Chem. Phys.* **2020**, *20* (10), 5887–5897.

(5) Wei, L.; Fu, P.; Chen, X.; An, N.; Yue, S.; Ren, H.; Zhao, W.; Xie, Q.; Sun, Y.; Zhu, Q.-F.; Wang, Z.; Feng, Y.-Q. Quantitative determination of hydroxymethanesulfonate (HMS) using ion chromatography and UHPLC-LTQ-Orbitrap mass spectrometry: A missing source of sulfur during haze episodes in Beijing. *Environ. Sci. Technol. Lett.* **2020**, *7* (10), 701–707.

(6) Liu, J.; Gunsch, M. J.; Moffett, C. E.; Xu, L.; El Asmar, R.; Zhang, Q.; Watson, T. B.; Allen, H. M.; Crounse, J. D.; St Clair, J.; Kim, M.; Wennberg, P. O.; Weber, R. J.; Sheesley, R. J.; Pratt, K. A. Hydroxymethanesulfonate (HMS) formation during summertime fog in an Arctic oil field. *Environ. Sci. Technol. Lett.* **2021**, *8* (7), 511–518.

(7) Campbell, J. R.; Battaglia, M., Jr.; Dingilian, K.; Cesler-Maloney, M.; St Clair, J. M.; Hanisco, T. F.; Robinson, E.; DeCarlo, P.; Simpson, W.; Nenes, A.; Weber, R. J.; Mao, J. Source and chemistry of hydroxymethanesulfonate (HMS) in Fairbanks, Alaska. *Environ. Sci. Technol.* **2022**, *56* (12), 7657–7667.

(8) Chen, C.; Zhang, Z.; Wei, L.; Qiu, Y.; Xu, W.; Song, S.; Sun, J.; Li, Z.; Chen, Y.; Ma, N.; Xu, W.; Pan, X.; Fu, P.; Sun, Y. The importance of hydroxymethanesulfonate (HMS) in winter haze episodes in North China Plain. *Environ. Res.* **2022**, *211*, No. 113093.

(9) Moch, J. M.; Dovrou, E.; Mickley, L. J.; Keutsch, F. N.; Liu, Z.; Wang, Y.; Dombek, T. L.; Kuwata, M.; Budisulistiorini, S. H.; Yang, L.; Decesari, S.; Paglione, M.; Alexander, B.; Shao, J.; Munger, J. W.; Jacob, D. J. Global importance of hydroxymethanesulfonate in ambient particulate matter: Implications for air quality. *J. Geophys. Res.: Atmos.* **2020**, *125* (18), No. e2020JD032706.

(10) Dovrou, E.; Lim, C. Y.; Canagaratna, M. R.; Kroll, J. H.; Worsnop, D. R.; Keutsch, F. N. Measurement techniques for identifying and quantifying hydroxymethanesulfonate (HMS) in an aqueous matrix and particulate matter using aerosol mass spectrometry and ion chromatography. *Atmos. Meas. Tech.* **2019**, *12* (10), 5303–5315.

(11) Dovrou, E.; Bates, K. H.; Moch, J. M.; Mickley, L. J.; Jacob, D. J.; Keutsch, F. N. Catalytic role of formaldehyde in particulate matter formation. *Proc. Natl. Acad. Sci. U.S.A.* **2022**, *119* (6), No. e2113265119.

(12) Lai, D.; Wong, Y. K.; Xu, R.; Xing, S.; Ng, S. I. M.; Kong, L.; Yu, J. Z.; Huang, D. D.; Chan, M. N. Significant conversion of organic sulfur from hydroxymethanesulfonate to inorganic sulfate and peroxydisulfate ions upon heterogeneous OH oxidation. *Environ. Sci. Technol. Lett.* **2023**, *10* (9), 773–778.

(13) Lai, D.; Schaefer, T.; Zhang, Y.; Li, Y. J.; Xing, S.; Herrmann, H.; Chan, M. N. Deactivating effect of hydroxyl radicals reactivity by sulfate and sulfite functional groups in aqueous phase—atmospheric implications for small organosulfur compounds. *ACS ES&T Air* **2024**, *1* (7), 678–689.

(14) Zhang, Q.; Zheng, Y.; Tong, D.; Shao, M.; Wang, S.; Zhang, Y.; Xu, X.; Wang, J.; He, H.; Liu, W.; Ding, Y.; Lei, Y.; Li, J.; Wang, Z.; Zhang, X.; Wang, Y.; Cheng, J.; Liu, Y.; Shi, Q.; Yan, L.; Geng, G.; Hong, C.; Li, M.; Liu, F.; Zheng, B.; Cao, J.; Ding, A.; Gao, J.; Fu, Q.; Huo, J.; Liu, B.; Liu, Z.; Yang, F.; He, K.; Hao, J. Drivers of improved PM<sub>2.5</sub> air quality in China from 2013 to 2017. *Proc. Natl. Acad. Sci. U.S.A.* **2019**, *116* (49), 24463–24469.

(15) Jiang, X.; Li, G.; Fu, W. Government environmental governance, structural adjustment and air quality: A quasi-natural experiment based on the Three-year Action Plan to Win the Blue Sky Defense War. *J. Environ. Manage.* **2021**, *277*, No. 111470.

(16) Geng, G.; Liu, Y.; Liu, Y.; Liu, S.; Cheng, J.; Yan, L.; Wu, N.; Hu, H.; Tong, D.; Zheng, B.; Yin, Z.; He, K.; Zhang, Q. Efficacy of China's clean air actions to tackle PM<sub>2.5</sub> pollution between 2013 and 2020. *Nat. Geosci.* **2024**, *17* (10), 987–994.

- (17) Lei, L.; Zhou, W.; Chen, C.; He, Y.; Li, Z.; Sun, J.; Tang, X.; Fu, P.; Wang, Z.; Sun, Y. Long-term characterization of aerosol chemistry in cold season from 2013 to 2020 in Beijing, China. *Environ. Pollut.* **2021**, *268*, No. 115952.
- (18) Zhou, W.; Gao, M.; He, Y.; Wang, Q.; Xie, C.; Xu, W.; Zhao, J.; Du, W.; Qiu, Y.; Lei, L.; Fu, P.; Wang, Z.; Worsnop, D. R.; Zhang, Q.; Sun, Y. Response of aerosol chemistry to clean air action in Beijing, China: Insights from two-year ACSM measurements and model simulations. *Environ. Pollut.* **2019**, *255*, No. 113345.
- (19) Li, H.; Cheng, J.; Zhang, Q.; Zheng, B.; Zhang, Y.; Zheng, G.; He, K. Rapid transition in winter aerosol composition in Beijing from 2014 to 2017: Response to clean air actions. *Atmos. Chem. Phys.* **2019**, *19* (17), 11485–11499.
- (20) Chen, Q.; Miao, R.; Geng, G.; Shrivastava, M.; Dao, X.; Xu, B.; Sun, J.; Zhang, X.; Liu, M.; Tang, G.; Tang, Q.; Hu, H.; Huang, R.-J.; Wang, H.; Zheng, Y.; Qin, Y.; Guo, S.; Hu, M.; Zhu, T. Widespread 2013–2020 decreases and reduction challenges of organic aerosol in China. *Nat. Commun.* **2024**, *15* (1), No. 4465.
- (21) Moch, J. M.; Dovrou, E.; Mickley, L. J.; Keutsch, F. N.; Cheng, Y.; Jacob, D. J.; Jiang, J.; Li, M.; Munger, J. W.; Qiao, X.; Zhang, Q. Contribution of hydroxymethane sulfonate to ambient particulate matter: a potential explanation for high particulate sulfur during severe winter haze in Beijing. *Geophys. Res. Lett.* **2018**, *45* (21), 11969–11979.
- (22) Wang, H.; Li, J.; Wu, T.; Ma, T.; Wei, L.; Zhang, H.; Yang, X.; Munger, J. W.; Duan, F.; Zhang, Y.; Feng, Y.; Zhang, Q.; Sun, Y.; Fu, P.; McElroy, M. B.; Song, S. Model simulations and predictions of hydroxymethanesulfonate (HMS) in the Beijing-Tianjin-Hebei region, China: Roles of aqueous aerosols and atmospheric acidity. *Environ. Sci. Technol.* **2024**, *58* (3), 1589–1600.
- (23) Campbell, J. R.; Battaglia, M.; Dingilian, K. K.; Cesler-Maloney, M.; Simpson, W. R.; Robinson, E. S.; DeCarlo, P. F.; Temime-Roussel, B.; D'Anna, B.; Holen, A. L.; Wu, J.; Pratt, K. A.; Dibb, J. E.; Nenes, A.; Weber, R. J.; Mao, J. Enhanced aqueous formation and neutralization of fine atmospheric particles driven by extreme cold. *Sci. Adv.* **2024**, *10* (36), No. eado4373.
- (24) Zhang, H.; Xu, Y.; Jia, L. Hydroxymethanesulfonate formation as a significant pathway of transformation of SO<sub>2</sub>. *Atmos. Environ.* **2023**, *294*, No. 119474.
- (25) Song, S.; Ma, T.; Zhang, Y.; Shen, L.; Liu, P.; Li, K.; Zhai, S.; Zheng, H.; Gao, M.; Moch, J. M.; Duan, F.; He, K.; McElroy, M. B. Global modeling of heterogeneous hydroxymethanesulfonate chemistry. *Atmos. Chem. Phys.* **2021**, *21* (1), 457–481.
- (26) Tilgner, A.; Schaefer, T.; Alexander, B.; Barth, M.; Collett, J. L., Jr.; Fahey, K. M.; Nenes, A.; Pye, H. O. T.; Herrmann, H.; McNeill, V. F. Acidity and the multiphase chemistry of atmospheric aqueous particles and clouds. *Atmos. Chem. Phys.* **2021**, *21* (17), 13483–13536.
- (27) Munger, J. W.; Tiller, C.; Hoffmann, M. R. Identification of Hydroxymethanesulfonate in fog water. *Science* **1986**, *231* (4735), 247–249.
- (28) Kok, G. L.; Gitlin, S. N.; Lazrus, A. L. Kinetics of the formation and decomposition of hydroxymethanesulfonate. *J. Geophys. Res.: Atmos.* **1986**, *91* (D2), 2801–2804.
- (29) Zhu, Y.; Li, H.; Xing, C.; Dong, X.; Liu, C.; Qin, X.; Wang, G.; Liu, Z.; Ding, Z.; Tian, M.; Deng, C.; Huang, K. Unraveling a Novel Formation Pathway of Hydroxymethanesulfonate (HMS) in the Marine Atmosphere. *J. Geophys. Res.: Atmos.* **2024**, *129* (23), No. e2024JD041936.
- (30) Reilly, J. E.; Rattigan, O. V.; Moore, K. F.; Judd, C.; Eli Sherman, D.; Dutkiewicz, V. A.; Kreidenweis, S. M.; Husain, L.; Collett, J. L. Drop size-dependent S(IV) oxidation in chemically heterogeneous radiation fogs. *Atmos. Environ.* **2001**, *35* (33), 5717–5728.
- (31) Zhao, M.; Shen, H.; Zhang, J.; Liu, Y.; Sun, Y.; Wang, X.; Dong, C.; Zhu, Y.; Li, H.; Shan, Y.; Mu, J.; Zhong, X.; Tang, J.; Guo, M.; Wang, W.; Xue, L. Carbonyl compounds regulate atmospheric oxidation capacity and particulate sulfur chemistry in the coastal atmosphere. *Environ. Sci. Technol.* **2024**, *58* (39), 17334–17343.
- (32) Xu, R.; Li, X.; Dong, H.; Lv, D.; Kim, N.; Yang, S.; Wang, W.; Chen, J.; Shao, M.; Lu, S.; Wu, Z.; Chen, S.; Guo, S.; Hu, M.; Liu, Y.; Zeng, L.; Zhang, Y. Field observations and quantifications of atmospheric formaldehyde partitioning in gaseous and particulate phases. *Sci. Total Environ.* **2022**, *808*, No. 152122.
- (33) Kang, Y.; Wang, Y.; Cheng, M.; Liu, B.; Yao, D.; Wang, Y.; Tang, G. Response of formaldehyde to meteorology in Beijing: Primary or secondary contributions. *J. Environ. Sci.* **2025**, *156*, 486–494.
- (34) Xu, Y.; Ma, T.; Duan, F.; Wang, S.; Jiang, J.; Cheng, Y.; Su, H.; An, T.; Ma, Y.; Kimoto, T.; Huang, T.; He, K. Existence of hydroxymethanesulfonate (HMS) during spring haze and sandstorm events in Beijing: Implications for a heterogeneous formation pathway on mineral aerosols. *Environ. Pollut.* **2025**, *366*, No. 125483.
- (35) Dingilian, K.; Hebert, E.; Battaglia, M., Jr.; Campbell, J. R.; Cesler-Maloney, M.; Simpson, W.; St Clair, J. M.; Dibb, J.; Temime-Roussel, B.; D'Anna, B.; Moon, A.; Alexander, B.; Yang, Y.; Nenes, A.; Mao, J.; Weber, R. J. Hydroxymethanesulfonate and sulfur(IV) in Fairbanks winter during the ALPACA study. *ACS ES&T Air* **2024**, *1* (7), 646–659.
- (36) Fountoukis, C.; Nenes, A. ISORROPIA II: a computationally efficient thermodynamic equilibrium model for K<sup>+</sup>–Ca<sup>2+</sup>–Mg<sup>2+</sup>–NH<sub>4</sub><sup>+</sup>–Na<sup>+</sup>–SO<sub>4</sub><sup>2-</sup>–NO<sub>3</sub><sup>-</sup>–Cl<sup>-</sup>–H<sub>2</sub>O aerosols. *Atmos. Chem. Phys.* **2007**, *7* (17), 4639–4659.
- (37) Nenes, A.; Pandis, S. N.; Weber, R. J.; Russell, A. Aerosol pH and liquid water content determine when particulate matter is sensitive to ammonia and nitrate availability. *Atmos. Chem. Phys.* **2020**, *20* (5), 3249–3258.
- (38) Song, S.; Nenes, A.; Gao, M.; Zhang, Y.; Liu, P.; Shao, J.; Ye, D.; Xu, W.; Lei, L.; Sun, Y.; Liu, B.; Wang, S.; McElroy, M. B. Thermodynamic Modeling Suggests Declines in Water Uptake and Acidity of Inorganic Aerosols in Beijing Winter Haze Events during 2014/2015–2018/2019. *Environ. Sci. Technol. Lett.* **2019**, *6* (12), 752–760.
- (39) Guo, H.; Sullivan, A. P.; Campuzano-Jost, P.; Schroder, J. C.; Lopez-Hilfiker, F. D.; Dibb, J. E.; Jimenez, J. L.; Thornton, J. A.; Brown, S. S.; Nenes, A.; Weber, R. J. Fine particle pH and the partitioning of nitric acid during winter in the northeastern United States. *J. Geophys. Res.: Atmos.* **2016**, *121* (17), 10355–10376.
- (40) Sun, Y.; Wang, Z.; Fu, P.; Jiang, Q.; Yang, T.; Li, J.; Ge, X. The impact of relative humidity on aerosol composition and evolution processes during wintertime in Beijing, China. *Atmos. Environ.* **2013**, *77*, 927–934.
- (41) Zheng, G. J.; Duan, F. K.; Su, H.; Ma, Y. L.; Cheng, Y.; Zheng, B.; Zhang, Q.; Huang, T.; Kimoto, T.; Chang, D.; Pöschl, U.; Cheng, Y. F.; He, K. B. Exploring the severe winter haze in Beijing: the impact of synoptic weather, regional transport and heterogeneous reactions. *Atmos. Chem. Phys.* **2015**, *15* (6), 2969–2983.
- (42) Boyce, S. D.; Hoffmann, M. R. Kinetics and mechanism of the formation of hydroxymethanesulfonic acid at low pH. *J. Phys. Chem.* **1984**, *88* (20), 4740–4746.
- (43) Deister, U.; Neeb, R.; Helas, G.; Warneck, P. Temperature dependence of the equilibrium CH<sub>2</sub>(OH)<sub>2</sub> + HSO<sub>3</sub><sup>-</sup> = CH<sub>2</sub>(OH)SO<sub>3</sub><sup>-</sup> + H<sub>2</sub>O in aqueous solution. *J. Phys. Chem.* **1986**, *90* (14), 3213–3217.
- (44) Olson, T. M.; Hoffmann, M. R. Hydroxyalkylsulfonate formation - its role as a S(IV) reservoir in atmospheric water droplets. *Atmos. Environ.* **1989**, *23* (5), 985–997.
- (45) Li, C.; Hammer, M. S.; Zheng, B.; Cohen, R. C. Accelerated reduction of air pollutants in China, 2017–2020. *Sci. Total Environ.* **2022**, *803*, No. 150011.
- (46) Wang, J.; Gao, J.; Che, F.; Wang, Y.; Lin, P.; Zhang, Y. Decade-long trends in chemical component properties of PM<sub>2.5</sub> in Beijing, China (2011–2020). *Sci. Total Environ.* **2022**, *832*, No. 154664.
- (47) Wu, Z.; Wang, Y.; Tan, T.; Zhu, Y.; Li, M.; Shang, D.; Wang, H.; Lu, K.; Guo, S.; Zeng, L.; Zhang, Y. Aerosol liquid water driven by anthropogenic inorganic salts: Implying its key role in haze formation over the North China Plain. *Environ. Sci. Technol. Lett.* **2018**, *5* (3), 160–166.
- (48) An, Z.; Huang, R.-J.; Zhang, R.; Tie, X.; Li, G.; Cao, J.; Zhou, W.; Shi, Z.; Han, Y.; Gu, Z.; Ji, Y. Severe haze in northern China: A synergy of anthropogenic emissions and atmospheric processes. *Proc. Natl. Acad. Sci. U.S.A.* **2019**, *116* (18), 8657–8666.



(49) Sun, Y.; Jiang, Q.; Wang, Z.; Fu, P.; Li, J.; Yang, T.; Yin, Y. Investigation of the sources and evolution processes of severe haze pollution in Beijing in January 2013. *J. Geophys. Res.: Atmos.* **2014**, *119*, 4380–4398.

(50) Duan, J.; Huang, R.-J.; Chang, Y.; Zhong, H.; Gu, Y.; Lin, C.; Hoffmann, T.; O'Dowd, C. Measurement report of the change of PM<sub>2.5</sub> composition during the COVID-19 lockdown in urban Xi'an: Enhanced secondary formation and oxidation. *Sci. Total Environ.* **2021**, 791, No. 148126.

(51) Cheng, Y.; Zheng, G.; Wei, C.; Mu, Q.; Zheng, B.; Wang, Z.; Gao, M.; Zhang, Q.; He, K.; Carmichael, G.; Pöschl, U.; Su, H. Reactive nitrogen chemistry in aerosol water as a source of sulfate during haze events in China. *Sci. Adv.* **2016**, *2* (12), No. e1601530.

(52) Song, S.; Gao, M.; Xu, W.; Shao, J.; Shi, G.; Wang, S.; Wang, Y.; Sun, Y.; McElroy, M. B. Fine-particle pH for Beijing winter haze as inferred from different thermodynamic equilibrium models. *Atmos. Chem. Phys.* **2018**, *18* (10), 7423–7438.

(53) Ding, J.; Zhao, P.; Su, J.; Dong, Q.; Du, X.; Zhang, Y. Aerosol pH and its driving factors in Beijing. *Atmos. Chem. Phys.* **2019**, *19* (12), 7939–7954.

The advertisement features a vertical strip on the left showing a 3D molecular model with various colored spheres (grey, orange, blue, green) connected by lines. The main background is dark blue. Text is in white and yellow. The CAS logo is at the bottom right.

**CAS BIOFINDER DISCOVERY PLATFORM™**

**ELIMINATE DATA  
SILOS. FIND  
WHAT YOU  
NEED, WHEN  
YOU NEED IT.**

A single platform for relevant,  
high-quality biological and  
toxicology research

**Streamline your R&D**

**CAS**  
A division of the  
American Chemical Society